Proceedings of Global Power and Propulsion Society
ISSN-Nr: 2504-4400
GPPS Xi'an21
18th – 20th October, 2021
www.gpps.global

GPPS-TC-2021-0145

Sequential ensemble multi-objective optimization algorithm and its application on the multi-working performance optimization of the variable cycle engine

Yifan Ye
Northwestern Polytechnical University
yyfan_@mail.nwpu.edu.cn
Xi'an, Shaanxi, China

Zhanxue Wang
Northwestern Polytechnical University
wangzx@nwpu.edu.cn
Xi'an, Shaanxi, China

Xiaobo Zhang
Northwestern Polytechnical University
zhangxb@nwpu.edu.cn
Xi'an, Shaanxi, China

ABSTRACT

The numerical design optimization is becoming more and more popular as the rapid development of computer technology. The efficient global optimization (EGO) algorithm is one of the most popular optimization algorithm used in the investigation of aerospace engineering systems in recent years. Many researches optimize several conflicting performance objectives by using the improved version of EGO in recent years. The EGO algorithm is a Kriging-assisted optimization algorithm. Wherein, the Kriging surrogate model is used to predict the performance objectives. Thus the accuracy of the Kriging surrogate model affects the EGO algorithm performance. The multi-surrogate technology can build an ensemble surrogate model by combining different individual surrogates. The ensemble model shows better accuracy than the other individual surrogate model. Thus, this paper proposes a sequential ensemble multi-objective optimization (SEMO). In the proposed algorithm, the ensemble model is used to generate the new sample points during the optimization process. Also, a new Pareto conserve strategy is proposed to enhance the accuracy of the optimal solution set. To verify the performance of SEMO, four well-known multi-objective optimization mathematical functions is considered in this paper. Further, SEMO algorithm is applied to the multi-working performance optimization of the variable cycle engine.

INTRODUCTION

The design optimization methods play an essential role in the investigation of design optimization of aerospace engineering systems. The surrogate-based optimization (SBO) algorithm is usually used in the investigation of aerospace engineering systems because of its high efficiency, such as engine performance optimization[1] [2], trajectory optimization[3][4], aerodynamic wing design optimization[5], and airfoil shape design optimization[6].

This paper considers the variable cycle engine (VCE) multi-working points performance optimization design. The variable cycle engine can meet different performance requirements under different flight conditions by adjusting its adjustable components. Thus the design optimization problem of the VCE is a multi-objective optimization problem. This problem is challenging to solve because there are many adjustable components in the VCE. The SBO algorithm is one of the most effective methods to solve this problem. Therefore, the investigation about the VCE multi-working points performance optimization method based on the surrogate model is proposed in this paper.

The efficient global optimization (EGO[7]) algorithm is one of the most popular SBO algorithm. Wherein, the Kriging surrogate model generated the new sample point per cycle optimization. It is an efficient way to improve the performance of EGO that improving the accuracy of the surrogate model. Some recent investigations proposed a multi-surrogate technology to improve the accuracy of the surrogate model. Wherein, several individual surrogate are combined by a weighted-sum formulation to build an ensemble surrogate model. Goel et al.[8] built an average ensemble surrogate model by using the data-based global error measure of individual surrogate model. Acar and Rais-Rohani[9] converted the weight factors calculation problem into an optimization problem. Then Viana et al.[10] calculated the weights by minimizing a new data-based global error measure, and solved this optimization problem by using Lagrange multipliers.

Thus, some recent investigations also prove that the performance of EGO algorithm can be further improved with replacing the Kriging surrogate model by the ensemble model. Ginsbourger et al.[11] proposed the EGO algorithm can be

assisted by using the ensemble of Kriging models. Ferreira and Serpa[12] proposed a least-squares ensemble model and apply this model in the EGO algorithm. The SBO algorithm based on the ensemble model has also been used in some engineering system designs, such as compressor blade shape optimization[13], reduction of helicopter vibration[14].

Motivating by these findings, a sequential ensemble multi-objective optimization (SEMO) is proposed in this paper. Which is a multi-objective SBO algorithm based on the ensemble surrogate model. And then a Pareto conserve strategy (PCS) is proposed to enhance the accuracy of the optimal solution set.

METHODOLOGY

The mathematical optimization formulation of VCE multi-working points optimization

VCE multi-working points optimization problem

The three working points performance optimization of a double-bypass VCE is considered in this paper. This optimization problem is a multi-objective optimization problem. It can be defined as:

$$\begin{aligned} &Obj \\ &Max\ F_{takeoff} \\ &Min\ SFC_{subsonic} \\ &Min\ SFC_{supersonic} \\ &s.t. \\ &F_{subsonic} = F_{subsonic,limit} \\ &F_{supersonic} = F_{supersonic,limit} \\ &N_{Fan} \le N_{Fan,limit} \\ &N_{CDFS} \le N_{CDFS,limit} \\ &N_{HPC} \le N_{HPC,limit} \\ &SM_{Fan} \ge SM_{Fan,limit} \\ &SM_{CDFS} \ge SM_{CDFS,limit} \\ &SM_{HPC} \ge SM_{HPC,limit} \\ &X_{\min} \le X \le X_{\max} \end{aligned} \quad . \tag{1}$$

where $F_{takeoff}$ is the thrust under the takeoff condition, and $SFC_{subsonic}$ is the specific fuel consumption under the subsonic cruise condition, and $SFC_{supersonic}$ is the specific fuel consumption under the supersonic cruise condition. These three parameters are the optimization objectives, and the others parameters are optimization constraints. $F_{subsonic}$ and $F_{supersonic}$ are the thrust values under two off-design conditions, the subsonic cruise condition and the supersonic cruise condition, N_{Fan}, N_{CDFS}, N_{HPC} are compressors' relative speeds, SM_{FAN}, SM_{CDFS}, SM_{HPC} are compressors' surge margin values; X represents the optimization variables.

Among all the constraints in the problem, the thrust constraints under the subsonic and supersonic cruise conditions are the most important. However, there is no efficient constraint handling method to deal with the equality constraint. Therefore, to reduce the solution difficulty, an adaptive simulation model is proposed in this paper. Wherein, the rotor speed is adjusted so that the thrust is equal to the given constraint value.

Figure 1 shows the flowchart of the proposed adaptive simulation model.

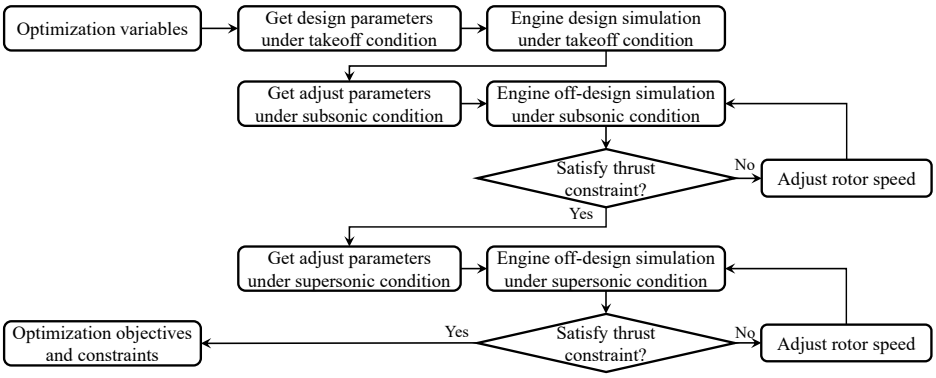

Figure 1 Flowchart of Adaptive Simulation Model

Sequential Ensemble Multi-Objective Optimization Algorithm

A multi-objective surrogate-based optimization algorithm named SEMO is proposed in this paper for the VCE multi-working points performance optimization. Wherein, the Ensemble of Least-Squares based RBF-networks (ELS-RBF) is used to assisted the traditional SBO algorithm. Meanwhile, the SEMO is augmented by using a PCS to obtain the better optimized Pareto solutions.

SEMO framework

The flowchart of the multi-objective version of the EGO algorithm (efficient global multi-objective optimization, EGMO) is shown in Figure 2, and the flowchart of the proposed SEMO algorithm is shown in Figure 3.

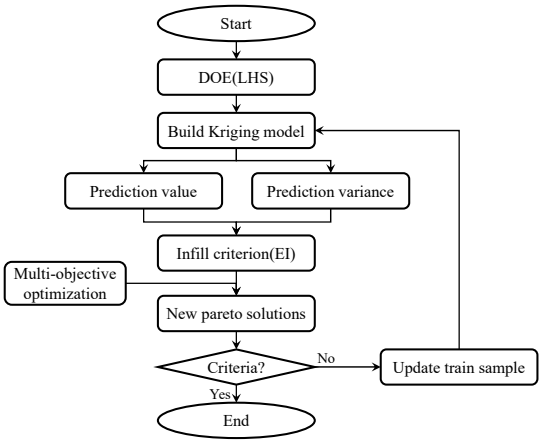

Figure 2 Flowchart of EGMO

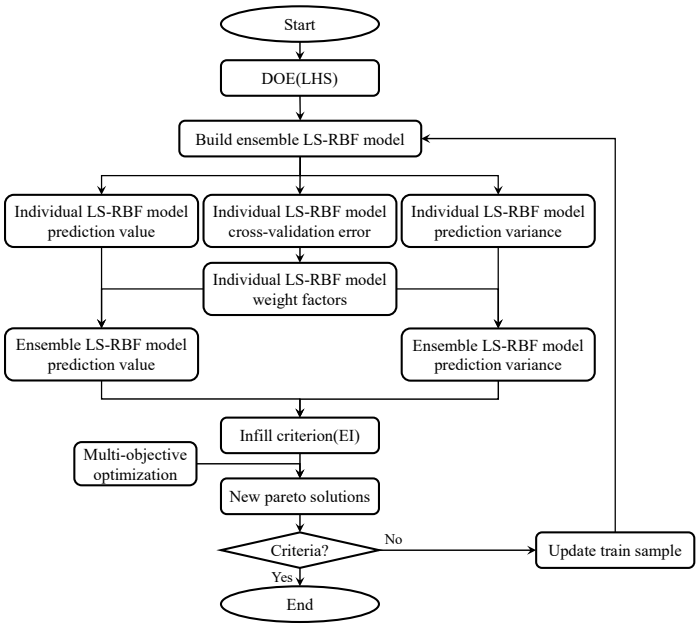

Figure 3 Flowchart of SEMO

In the EGMO and SEMO algorithm, the new sample points are generated based on the maximization of the EI. After gaining the new sample points, the simulation model is used to calculate the corresponding true responses. The NSGA-II[15] algorithm is used to maximize the EI in this paper. In the EGMO algorithm, the Kriging surrogate model prediction value and prediction variance are used to construct the EI per optimization cycle. In the proposed SEMO algorithm, the ELS-RBF model prediction value and prediction variance is used to construct the EI per optimization cycle.

The individual LS-RBF model can be expressed as:

$$\mathbf{y} = \mathbf{Y}\mathbf{a} + \varepsilon \,. \tag{2}$$

Where $\mathbf{y}=[y_1,y_2,\ldots y_N]^T$, $\mathbf{Y}=[y'_1(\mathbf{x}_i), y'_2(\mathbf{x}_i),\ldots,y'_M(\mathbf{x}_i)]^T$, $\mathbf{a}=[a_1,a_2,\ldots,a_M]^T$, for N sampling points and M basis functions. The standard least squares estimator for $\mathbf{a}$ is calculated by:

$$\mathbf{w} = \left(\mathbf{Y}^T\mathbf{Y}\right)^{-1}\mathbf{Y}^T\mathbf{y} \,. \tag{3}$$

The individual LS-RBF model prediction variance is calculated by:

$$\begin{aligned} s^2(\mathbf{x}) &= \sigma^2\left[\mathbf{y}'(\mathbf{x})\right]^T\left(\mathbf{Y}^T\mathbf{Y}\right)^{-1}\mathbf{y}'(\mathbf{x}) \\ \sigma^2 &= \frac{\mathbf{y}'_{\mathrm{mod}}{}^T\mathbf{y}'_{\mathrm{mod}} - \mathbf{w}^T\mathbf{Y}\mathbf{y}'_{\mathrm{mod}}}{N - n_v} \end{aligned} \,. \tag{4}$$

Where $\mathbf{y}'(\mathbf{x})=[\,\mathbf{y}'_1(\mathbf{x}), \mathbf{y}'_2(\mathbf{x}),\ldots, \mathbf{y}'_M(\mathbf{x})]$, $\mathbf{y}'_{\mathrm{mod}}=[\,\mathbf{y}'_{\mathrm{mod}}(\mathbf{x}_1), \mathbf{y}'_{\mathrm{mod}}(\mathbf{x}_2),\ldots, \mathbf{y}'_{\mathrm{mod}}(\mathbf{x}_N)]^T$.

The ELS-RBF model is constructed by:

$$y'_e(\mathbf{x}) = \sum_{i=1}^{m} w_i(\mathbf{x})\, y'_{\mathrm{mod},i}(\mathbf{x}) \,. \tag{5}$$

where $y'_e(\mathbf{x})$ is the ELS-RBF model, $y'_{\mathrm{mod},i}(\mathbf{x})$ is the ith individual LS-RBF model, and the calculation method of weight factor $w_i(\mathbf{x})$ in [10] is used in this paper. The ELS-RBF model variance can be calculated as:

$$s_e^2(\mathbf{x}) = \sum_{i=1}^{m} w_i(\mathbf{x})\, s_i^2(\mathbf{x}) \,. \tag{6}$$

where $s^2_e(\mathbf{x})$ is the ELS-RBF model variance, $s^2_i(\mathbf{x})$ is the ith individual LS-RBF model variance.

The new sample points are gained by using the EI infill criterion. Wherein, the multi-objective evolution optimization algorithm is used to solve this sub-optimization problem. The advantage of evolutionary optimization algorithm is that it has strong global convergence. However, local convergence rate of evolutionary optimization algorithm is poor. Thus, this paper also proposes a PCS to improve the accuracy of optimized Pareto solutions.

Pareto conserve strategy

The proposed PCS is an additional mechanism for the evolution optimization algorithm. In the SEMO loop, the PCS is conducive to improve the solution quality obtained by evolution optimization algorithm. The proposed PCS divides the optimization process into two periods. The different population initialization method is used in different two periods for different optimization purposes. In the first period of the optimization process, the optimization purpose is to explore the global optimal solutions. Thus, the current solutions are randomly selected for initializing the initial populations of the NSGA-II. The second period of optimization process begins when the number of optimization steps exceeds half of the maximum number of optimization steps.

In the second period of the optimization process, the optimization purpose is to exploit the optimized Pareto solutions. Thus, the current Pareto solutions are used for initializing the initial populations of the NSGA-II to improve the algorithm local exploitation ability. The initialization strategy first divides the current solutions into different nondominated front according to the Pareto domination. The solutions in the first nondominated front are better than those in the second or higher nondominated front in terms of the Pareto domination. If the number of solutions in the first nondominated front is larger than the number of initial populations, these solutions are randomly selected for initializing the initial populations. If the number of solutions in the first nondominated front is less than the number of initial populations, these solutions are all selected for initializing the initial populations, and the solutions in the second or higher nondominated front are randomly selected for initializing the initial populations.

Test Functions and Optimization Problem

Test functions

To verify the effect of the proposed algorithm, four well-known example problems were considered.

- ZDT1

$$\begin{cases} \min\ f_1(\boldsymbol{X}) = x_1 \\ \min\ f_2(\boldsymbol{X}) = g(\boldsymbol{X})\left(1-\sqrt{f_1(\boldsymbol{X})/g(\boldsymbol{X})}\right) \\ g(\boldsymbol{X}) = 1+\dfrac{9\sum_{i=2}^{n} x_i}{(n-1)}, 0 \le x_i \le 1 (i=1,2,\cdots,n) \end{cases} . \tag{7}$$

- ZDT2

$$\begin{cases} \min\ f_1(\boldsymbol{X}) = x_1 \\ \min\ f_2(\boldsymbol{X}) = g(\boldsymbol{X})\left(1-\left(f_1(\boldsymbol{X})/g(\boldsymbol{X})\right)^2\right) \\ g(\boldsymbol{X}) = 1+\dfrac{9\sum_{i=2}^{n} x_i}{(n-1)}, 0 \le x_i \le 1 (i=1,2,\cdots,n) \end{cases} . \tag{8}$$

- ZDT3

$$\begin{cases} \min\ f_1(\boldsymbol{X}) = x_1 \\ \min\ f_2(\boldsymbol{X}) = g(\boldsymbol{X})\left(1-\left(f_1(\boldsymbol{X})/g(\boldsymbol{X})\right)-\left(f_1(\boldsymbol{X})/g(\boldsymbol{X})\right)\sin(10\pi x_1)\right) \\ g(\boldsymbol{X}) = 1+\dfrac{9\sum_{i=2}^{n} x_i}{(n-1)}, 0 \le x_i \le 1 (i=1,2,\cdots,n) \end{cases} . \tag{9}$$

- DTLZ5

$$\begin{cases} \min\ f_1(\boldsymbol{X}) = (1+g(\boldsymbol{X}_M))\cos(\theta_1 \pi/2)\cdots\cos(\theta_{M-2}\pi/2)\cos(\theta_{M-1}\pi/2) \\ \min\ f_2(\boldsymbol{X}) = (1+g(\boldsymbol{X}_M))\cos(\theta_1 \pi/2)\cdots\cos(\theta_{M-2}\pi/2)\sin(\theta_{M-1}\pi/2) \\ \min\ f_3(\boldsymbol{X}) = (1+g(\boldsymbol{X}_M))\cos(\theta_1 \pi/2)\cdots\sin(\theta_{M-2}\pi/2) \\ \quad\vdots \\ \min\ f_M(\boldsymbol{X}) = (1+g(\boldsymbol{X}_M))\sin(\theta_1 \pi/2) \\ \theta_i = \dfrac{\pi}{4(1+g(\boldsymbol{X}_M))}(1+2g(\boldsymbol{X}_M)x_i)(i=2,3,\cdots,(M-1)) \\ g(\boldsymbol{X}_M) = \sum_{x_i \in \boldsymbol{X}_M}(x_i-0.5)^2, 0 \le x_i \le 1 (i=1,2,\cdots,n) \end{cases} . \tag{10}$$

For the ZDT1, ZDT2, and ZDT3, the eight-variable model (n=8) is considered. For the DTLZ5, the six-variable and three-objective model (n=6, M=3) is considered. The Latin hypercube sampling (LHS) technique is used in this paper to gain the initial sample set. The size of initial sample set for ZDT1, ZDT2, and ZDT3 is 60. The size of initial sample set

for DTLZ5 is 40. The LHS program is run with the maximum iteration number of 1000 for all test functions. The maximum optimization step for ZDT1, ZDT2, and ZDT3 is 300, while maximum optimization step for DTLZ5 is 200.

Optimization problem

The three working points performance optimization of a three-bypass VCE is considered in this paper. The engine simulation model was formed using the aero-engine simulation system proposed in [16].The component-based numerical model of VCE used in this paper is shown in Figure 4. As shown in Figure 4, this model consists of an inlet, a fan stage on blade (FLADE), a fan, a mode select valve (MSV), a core-driven fan stage (CDFS), a high-pressure compressor (HPC), a burner, a high-pressure turbine (HPT), a low-pressure turbine (LPT), a forward variable area bypass injector (FVABI), a rear variable area bypass injector (RVABI), two nozzles, and three ducts.

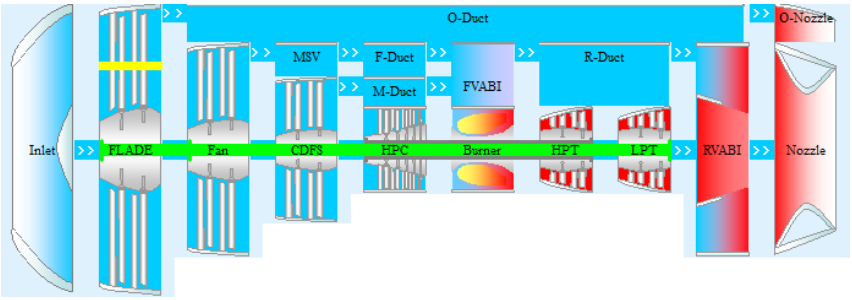

Figure 4 Component-based Numerical Model of VCE

The flight conditions and engine operation modes of the three working points are shown in Table 1.

Table 1 Flight Conditions and Engine Operation Modes of Three Working Points

	Flight altitude (m)	*Flight Mach*	*MSV*
Takeoff condition	0	0	Open
Subsonic condition	10668	0.95	Open
Supersonic condition	16306.8	2.32	Closed

The optimization variables and their ranges are shown in Table 2.

Table 2 Optimization Variables' Ranges

Variable name	*Initial value*	*Low limit*	*Up limit*
FLADE design pressure ratio	1.5	1.2	2
Fan design bypass ratio	0.5	0.1	1
Fan design pressure ratio	2	1.2	4
CDFS design bypass ratio	0.3	0.1	1
CDFS design pressure ratio	1.5	1.1	1.8
HPC design pressure ratio	8	7	10
Burner outlet temperature (K)	1800	1600	2000
FLADE inlet guide vane angle (°)	0	0	10
CDFS inlet guide vane angle (°)	0	-45	0
HPC inlet guide vane angle (°)	0	-5	5
LPT nozzle area (%)	100	70	130
FVABI inner duct area (%)	0	-50	100
RVABI inner duct area (%)	0	-50	100
FLADE nozzle area (m^2)	0.05	0.04	0.07
Nozzle zrea (m^2)	0.3	0.2	0.4

The optimization constraint parameters are shown in Table 3.

Table 3 Optimization Constraint Parameters

Constraint parameters name	*Limit value*
Fsubsonic,limit (kgf)	1500
Fsupersonic,limit (kgf)	1800
NFan (%)	105
NCDFS (%)	105
NHPC (%)	105
SMFan,limit (%)	10
SMCDFS,limit (%)	10
SMHPC,limit (%)	10

The LHS technique is used to gain the initial sample set. The size of initial sample set is 160. The LHS program is run with the maximum iteration number of 1000. The maximum optimization step is 800.

RESULTS AND DISCUSSION

Figure 5 shows the boxplots of the Inverted Generational Distance (IGD) of the optimization results obtained by EGMO, SEMO, and SEMO-PCS. It can be seen from the figure that the SEMO algorithm performs better than the EGMO algorithm for all test functions. Thus using the ELS-RBF model improves the result quality obtained by SBO algorithm. The SEMO-PCS algorithm performs better than the SEMO algorithm for all test functions. This indicates that the PCS is beneficial to further improve the result quality obtained by SEMO by combining different initialization strategies. Figure 6 shows the plots of the final optimization solutions in the objective space on test functions. It can be seen from the figure that the Pareto front obtained by SEMO and SEMO-PCS closes to the true Pareto front. The distribution of optimized Pareto solutions obtained by SEMO-PCS is better than that obtained by SEMO. This indicates that the PCS can improve the optimized Pareto solutions quality.

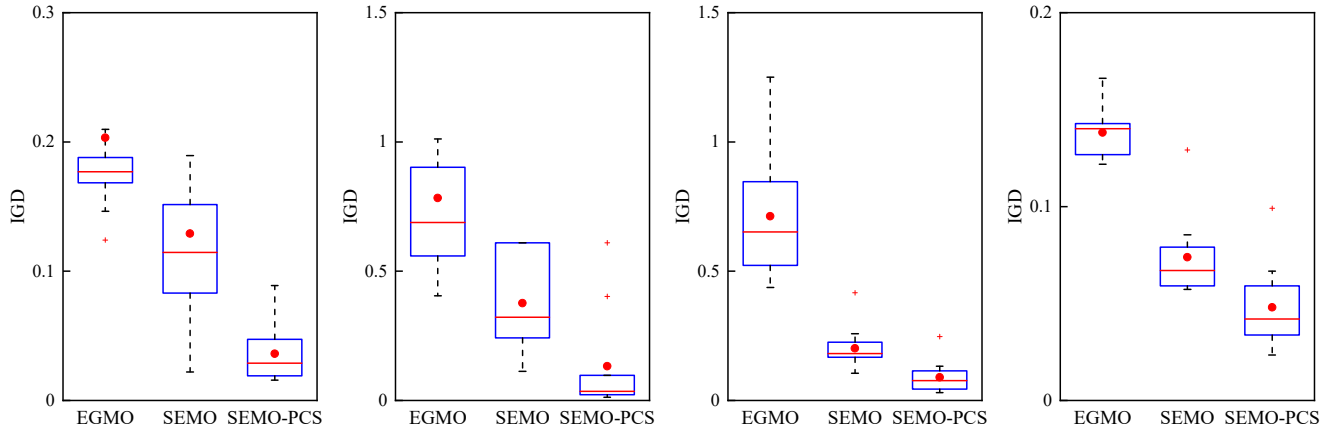

(a) ZDT1 (b) ZDT2 (c) ZDT3 (d) DTLZ5

Figure 5 Boxplot of The IGD Values of The Final Optimization Solutions on Test Functions

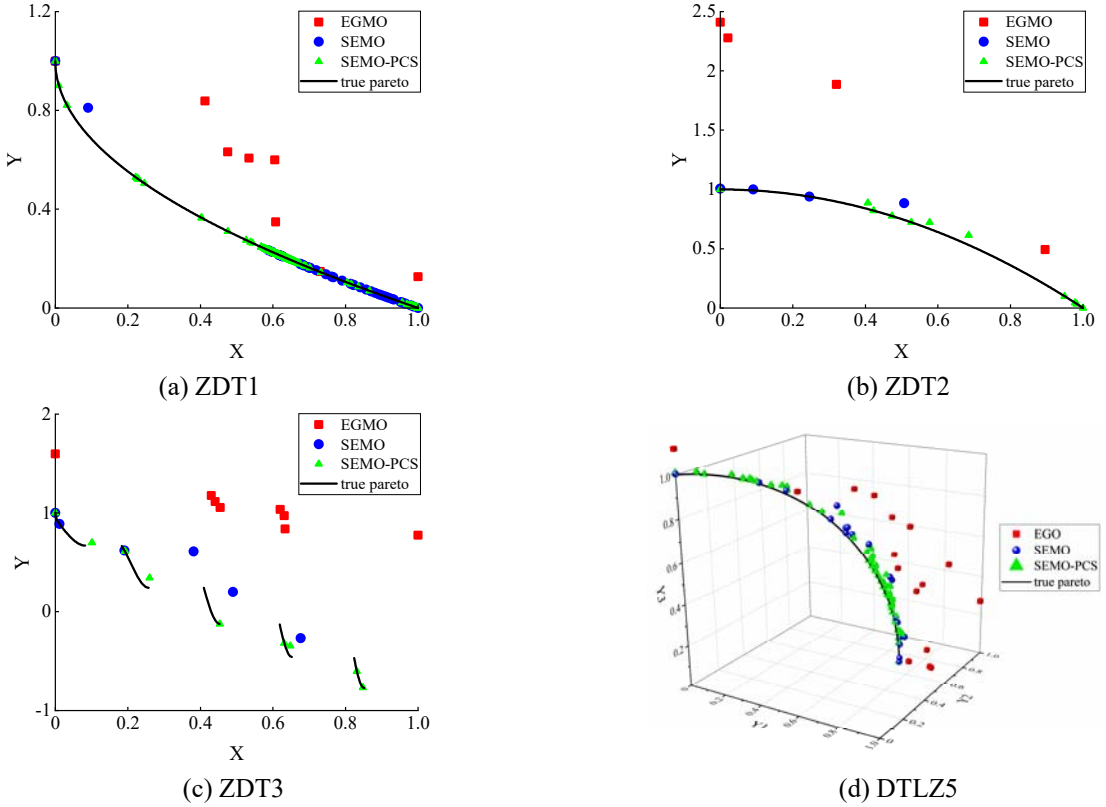

(a) ZDT1 (b) ZDT2

(c) ZDT3 (d) DTLZ5

Figure 6 Plots of The Final Optimization Solutions in The Objective Space on Test Functions

Figure 7 shows the Pareto front of the optimized VCE multi-working points performance. Wherein, two boundary solutions and an intermediate solution are selected from the Pareto solutions, and the optimization parameters and objectives values are shown in Table 4.

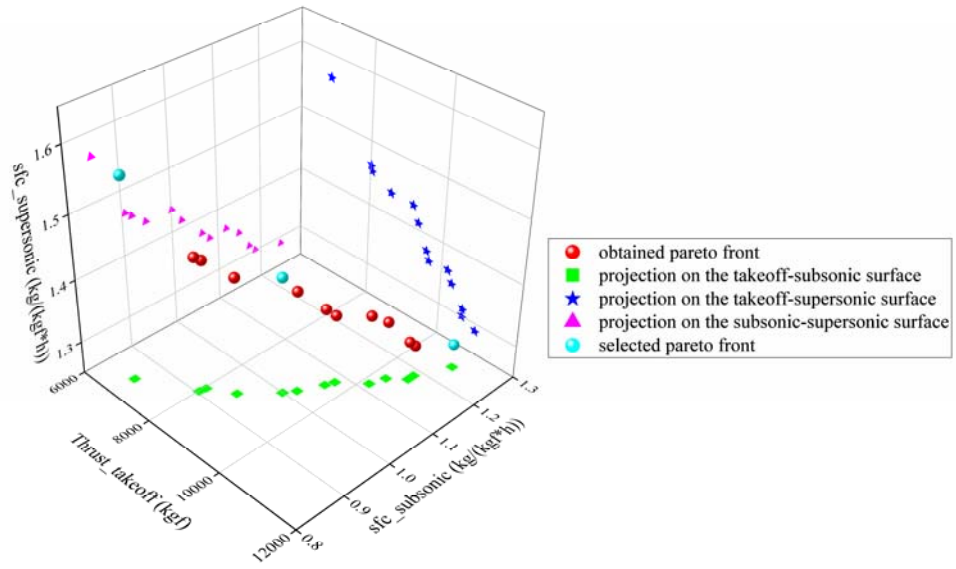

Figure 7 Pareto Front of The Optimized VCE Multi-working Points Performance

Table 4 Three Solutions Selected from The Pareto Solutions

Optimization parameters	*Solution. A*	*Solution. B*	*Solution. C*
Takeoff condition			
FLADE design pressure ratio	2	2	1.925
Fan design bypass ratio	0.1	0.363	0.872
Fan design pressure ratio	4	3.453	3.286
CDFS design bypass ratio	0.10288	0.103	0.249
CDFS design pressure ratio	1.1	1.1	1.160
HPC design pressure ratio	7	9.032	9.987
Burner outlet temperature (K)	2000	1896	1886
Subsonic cruise condition			
FLADE inlet guide vane angle	3.502	4.927	5.223
CDFS inlet guide vane angle (°)	0	0	-5.243
HPC inlet guide vane angle	-3.751	2.242	-2.858
LPT nozzle area (%)	130	130	130
FVABI inner duct area (%)	44.28	60	-16.64
RVABI inner duct area (%)	-30.245	-50	6.035
FLADE nozzle area (m^2)	0.047	0.065	0.044
Nozzle zrea (m^2)	0.292	0.2	0.334
Supersonic cruise condition			
CDFS inlet guide vane angle (°)	-21.776	-17.676	-24.922
HPC inlet guide vane angle (°)	-0.356	-5	-0.676
LPT nozzle area (%)	114.6	103.8	104.3
FVABI inner duct area (%)	38.76	60	13.48
RVABI inner duct area (%)	28.65	3.46	8.955
Nozzle zrea (m^2)	0.363	0.4	0.300
Optimization objectives			
$F_{takeoff}$ *(kgf)*	10961.4	9174.0	6852.6
$SFC_{subsonic}$ *(kg/(kgf*h))*	1.247	0.999	0.849
$SFC_{supersonic}$ *(kg/(kgf*h))*	1.288	1.434	1.565

It can be seen from Picture 6 and Table 4 that as the $F_{takeoff}$ increases, the $SFC_{subsonic}$ increases, the $SFC_{supersonic}$ decreases. The design bypass ratio of solutions with high $F_{takeoff}$ is lower than that of solutions with low $F_{takeoff}$. The design pressure ratio of solution with high $F_{takeoff}$ is higher than that of solutions with low $F_{takeoff}$. The design burner outlet temperature of solution with high $F_{takeoff}$ is higher than that of solutions with low $F_{takeoff}$.

The high design bypass ratio benefits the *SFC* under off-design conditions but hurts the *F* under the off-design conditions. The *SFC* under the off-design conditions decreases as the design bypass increases. Meanwhile the *F* under the off-design conditions decreases. In order to meet the thrust constraints under the off-design conditions, the adjustable

parameters are adjusted, and then *SFC* may increases. Thus, whether increasing design bypass ratio is beneficial to the *SFC* under the off-conditions depends on the thrust constraint.

In general, the thrust constraint under the subsonic cruise condition is easier to satisfy than that under the supersonic cruise condition. As the design bypass ratio increases, the thrust constraint under the subsonic cruise condition is still easy to satisfy. Thus the SFC under the subsonic cruise condition decreases. However, as the design bypass ratio increases, the thrust constraint under the supersonic cruise condition becomes harder to satisfy. To satisfy the thrust constraint, the adjustable components are adjusted to increase the thrust and then the SFC decreases.

CONCLUSIONS

A new multi-objective surrogate-based optimization algorithm named SEMO is proposed in this paper. In the SEMO algorithm, the ensemble surrogate model is used to assist the multi-objective optimization algorithm, and a PCS is also used to enhance the accuracy of the optimal solution set. The proposed SEMO algorithm is applied to four well-known mathematical functions and the multi-working performance optimization of the VCE. Some conclusions can be reached as:

1. Using the ELS-RBF is beneficial to the results quality obtained by SBO algorithm. And the PCS can benefit the SEMO algorithm performance by using different initialization strategy in different optimization periods.
2. As the thrust under the design condition decreases the design bypass ratio increases. This leads to the thrust constraint under the supersonic cruise condition become harder to satisfy. Thus the $SFC_{subsonic}$ increases, the $SFC_{supersonic}$ decreases.

REFERENCES

[1] Patnaik, S., Guptill, J., Hopkins, D. and Lavelle, T. (2001). Optimization for aircraft engines with regression and neural-network analysis approximators. *Journal of Propulsion and Power*, 17(1), pp. Jan-Feb.

[2] Pastrone, D. and Sentinella, M. (2009). Multi-objective optimization of rocket-based combined-cycle engine performance using a hybrid evolutionary algorithm. *Journal of Propulsion and Power*, 25(5), pp. Sep-Oct.

[3] Peng, H., Yang, C., Li, Y., Zhang, S. and Chen, B. (2013). Surrogate-based parameter optimization and optimal control for optimal trajectory of halo orbit rendezvous. *Aerospace Science and Technology*, 26, pp. 176-184.

[4] An, K., Gou, Z., Xu, X. and Huang, W. (2020). A framework of trajectory design and optimization for the hypersonic gliding vehicle. *Aerospace Science and Technology*, 106, pp. 106100.

[5] Bartoli, N., Lefebvre, T., Dubreuil, S., Olivanti, R., Priem, R., Bons, N., Martins, J. and Morlier, J. (2019). Adaptive modeling strategy for constrained global optimization with application to aerodynamic wing design. *Aerospace Science and Technology*, 90, pp. 85-102.

[6] He, Y., Sun, J., Song, P., Wang, X. and Usmani, A. (2020). Preference-driven Kriging-based multiobjective optimization method with a novel multipoint infill criterion and application to airfoil shape design. *Aerospace Science and Technology*, 96, pp. 105555.

[7] Jones, D., Schonlau, M. and Welch W. (1998). Efficient global optimization of expensive black-box functions. *Journal of Global Optimization*, 13(4), pp. 455-492.

[8] Goel, T., Haftka, R., Shyy, W., and Queipo, Q. (2007). Ensemble of surrogates. *Structural and Multidisciplinary Optimization*, 33, pp. 199-216.

[9] Acar, E. and Rais-Rohani, M. (2009). Ensemble of metamodels with optimized weight factors. *Structural and Multidisciplinary Optimization*, 37, pp. 279-294.

[10] Viana, F., Haftka, R. and Steffen, V. (2009). Multiple surrogates: how cross-validation errors help us to obtain the best predictor. *Structural and Multidisciplinary Optimization*, 39, pp. 439-457.

[11] Ginsbourger, D., Helbert, C. and Carraro, L. (2008). Discrete mixtures of kernels for Kriging-based optimization. *Quality and Reliabiliy Engineering International*, 24(6), pp. 681-691.

[12] Ferreira, W. and Serpa A. (2018). Ensemble of metamodels: Extensions of the least squares approach to efficient global optimization. *Structural and Multidisciplinary Optimization*, 57, pp. 131-159.

[13] Samad, A. and Kim K. (2008). Multiple surrogate modeling for axial compressor blade shape optimization. *Journal of Propulsion and Power*, 24(2), pp. 302-310.

[14] Glaz, B., Goel, T., Liu, L. and Haftka R. (2009). Multiple-surrogate approach to helicopter rotor blade vibration reduction. *AIAA Journal*, 47(1), pp. 271-282.

[15] Deb, K., Pratap, A., Agarwal, S. and Meyarivan T. (2002). A fast and elitist multiobjective genetic algorithm: NSGA-II. *IEEE Transactions on Evolutionary Computation*, 6(2), pp. 182-197.

[16] Zhang, X., Wang, Z., Zhou, L. and Liu, Z. (2016). Multidisciplinary design optimization on conceptual design of aero-engine. *International Journal of Turbo and Jet Engines*, 33, pp. 195-208.

ACKNOWLEDGMENTS

The authors would like to express their gratitude for the financial support of the National Natural Science Foundation of China (Nos. 52076180, 51876176 and 51906204) and National Science and Technology Major Project (J2019-I-0021-0020).